مجلة جامعة الزاوية للعلوم الطبيعية
University of Zawia Journal of Natural Sciences *(UZJNS)*
https://journals.zu.edu.ly/index.php/UZJNS ISSN: 3078-4999

Evaluation of Some Selective Surfaces Used for Solar Thermal Conversion Using the Calorimetric Method

Ali S Lahwal [a]

[a]*Department of General, Faculty of Natural Resources, University of Zawia, Zawia, Libya.*

** Corresponding email address: a.lahwal@zu.edu.ly*

Received 09 Jan 2026 | Accepted 02 Apr 2026 | Available online 14 Apr 2026 | DOI: 10.26629/uzjns.2026.04

A B S T R A C T

Knowledge of the selective radiative properties of surfaces is essential for the proper design of solar thermal collectors. Experimental results must directly reflect the conditions under which a surface will operate in order to accurately evaluate selective coatings for potential use in solar collectors. To achieve this, an instrument based on calorimetric techniques has been developed. It measures the solar absorptivity (α) and infrared (IR) emissivity (ε) of surfaces. These measurements determine the spectral selectivity of surfaces and assess their suitability for solar energy applications. The absorptivity (α) and total hemispherical emissivity (ε) are calculated as functions of temperature is measured by observing the rate at which a thermally isolated sample in an evacuated chamber heats up under real or simulated solar radiation. Emissivity is determined by measuring the rate at which the sample cools when shaded. These parameters allow comparison of the relative efficiencies of different surfaces over a range of operating temperatures. A graphite sheet was used as a blackbody reference to calibrate the instrument, and it was found that its absorptivity and emissivity are nearly equal, with values of approximately 0.94. Two additional samples were tested: a copper selective surface coated with aluminum and painted black, and an aluminum surface with V-grooving coated with a selective black paint. The results indicate that the copper-based surface is more suitable for solar collector applications than the aluminum surface, owing to the significant difference between its absorptivity and emissivity ($\alpha = 0.95, \varepsilon = 0.25$), which leads to higher thermal efficiency.

Keywords: *Selective surface, Absorptivity, Emissivity, Calorimeter, Black body, Solar energy, Solar collectors, Thermal conversion.*

تقييم بعض الاسطح الانتقائية المستخدمة في المجمعات الشمسية الحرارية باستخدام طريقة الكالوري ميتر الشمسي

علي الصادق الأحول [a]

[a]*القسم العام، كلية الموارد الطبيعية، جامعة الزاوية، الزاوية، ليبيا.*

الملخص

تُعدّ معرفة الخصائص الإشعاعية الانتقائية للأسطح أمرًا أساسيًا للتصميم السليم لمجمّعات الطاقة الشمسية الحرارية. ويجب أن تعكس النتائج التجريبية بشكل مباشر ظروف التشغيل الفعلية للسطح، وذلك من أجل التقييم الدقيق للطلاءات الانتقائية المرشّحة للاستخدام في المجمّعات الشمسية. ولهذا الغرض، تم تطوير جهاز يعتمد على تقنيات القياس الحراري (الكالوريمترية) لقياس الامتصاصية الشمسية ($\boldsymbol{\alpha}$) والانبعاثية في نطاق الأشعة تحت الحمراء ($\boldsymbol{\varepsilon}$) للأسطح. تُستخدم هذه القياسات لتحديد الانتقائية الطيفية للأسطح وتقييم مدى ملاءمتها لتطبيقات الطاقة الشمسية. ويتم حساب الامتصاصية ($\boldsymbol{\alpha}$) والانبعاثية الكلية نصف الكروية ($\boldsymbol{\varepsilon}$) كدوال في درجة الحرارة، وذلك من خلال قياس معدل ارتفاع درجة حرارة عينة معزولة حراريًا داخل حجرة مفرغة عند تعريضها لإشعاع شمسي حقيقي أو مُحاكى، وكذلك قياس معدل تبريدها عند حجب الإشعاع عنها. وتُمكّن هذه المعاملات من مقارنة الكفاءات النسبية لأسطح مختلفة عبر نطاق من درجات حرارة التشغيل.

استُخدمت صفيحة من الغرافيت كمرجع جسم أسود لمعايرة الجهاز، وتبيّن أن امتصاصيتها وانبعاثيتها متقاربتان جدًا، حيث بلغت قيمتهما نحو 0.94. كما تم اختبار عينتين إضافيتين: سطح نحاسي انتقائي مطلي بالألمنيوم ومطلي بطلاء أسود، وسطح من الألمنيوم ذو أخاديد على شكل حرف V مطلي بطلاء أسود انتقائي. وأظهرت النتائج أن السطح القائم على النحاس أكثر ملاءمة لتطبيقات المجمّعات الشمسية من سطح الألمنيوم، وذلك بسبب الفرق الكبير بين امتصاصيته وانبعاثيته مما يؤدي إلى كفاءة حرارية أعل$\boldsymbol{\alpha = 0.95, \varepsilon = 0.25}$ ى() ، مما يؤدي إلى كفاءة حرارية أعلى.

الكلمات المفتاحية: *السطح الانتقائي، الامتصاصية، الانبعاثية، كالوري ميتر، الجسم الاسود، الطاقة الشمسية، المجمعات الشمسية، التحويل الحراري.*

1. Introduction

The sun is an important source of energy. This energy is produced in the interior of the solar sphere, at temperatures of many millions of degrees. It must transfer out to the surface and then be radiated into space before arriving at the earth. The solar constant intensity, I_{sol}, is the energy from the sun, per unit time, received on a unit area of surface perpendicular to the radiation, in space, at the earth's mean distance from the sun. Until recently, estimates of the solar constant intensity had to be made from ground-based measurements of solar radiation after it had been transmitted through the atmosphere, and thus in part absorbed and scattered by components of the atmosphere. Extrapolations from high mountains had to be based on estimates of atmospheric transmission in various portions of the solar spectrum. Pioneering studies were done by C. G. Abbot and his colleagues at the Smithsonian Institution. These studies and later measurements from rockets were summarized [1]; Abbot's value of the solar constant intensity of 1322 W/m², was revised upward by Johnson to 1395 W/m². More recently, the availability of very high-altitude aircraft, balloons, and spacecraft has permitted direct measurements of solar intensity outside most or all of the earth's atmosphere. These measurements have been reviewed and summarized, and a new standard value of the solar constant proposed as 1353 W/m² [2]. The solar collector is the essential item of equipment which transforms solar radiation energy to some other useful energy form. A solar collector differs in several respects from more conventional heat exchangers. The latter usually accomplish a fluid-to-fluid exchange with high heat transfer rates and with radiation as an unimportant factor. In the solar collector, energy transfer is from a distant source of radiant energy to fluid. Without optical concentration, the flux of incident radiation is, at best, about 1100 W/m² and is variable [3]. Solar collectors may be used with or without radiation concentration. Use of solar selective coatings enhances the collector's performance significantly. There is a need to develop a cost-effective method to produce the coating on the absorber surface. These coatings could not be commercialized due to their high cost, low productivity, and complexity in processes [4]. For flat-plate collectors the area absorbing solar radiation is the same as the area intercepting solar radiation. The important parts of a typical flat-plate solar collector are the "black" solar energy-absorbing surface, which transferring the absorbed energy to a fluid; envelopes transparent to solar radiation over the solar absorber surface which reduce conduction losses as the geometry of the system permits. Flat-plate collectors are usually, although not always, mounted in a stationary position (e.g., as an integral part of a wall or roof structure in solar house heating) with an orientation optimized for the location in question for the time of year in which the solar device is intended to operate. In their most common forms, they are air or water heaters or low-pressure steam generators.

Focusing collectors usually have concave reflectors to concentrate the radiation falling on the total area of the reflector onto a heat exchanger of smaller surface area, thereby increasing the energy flux. Flat-plate collectors can be designed for applications requiring energy delivery at moderate temperatures, up to perhaps 100 °C above ambient temperature. They have the advantages of using both beam and diffuse solar radiation, not requiring orientation toward the sun, and requiring little maintenance. They are mechanically simpler than the concentrating reflectors, absorbing surfaces, and orientation devices of focusing collectors. The principle present applications of these units are in solar water heating systems, while potential uses include building heating and air conditioning. Focusing collectors utilize optical systems reflectors or refractors to increase the intensity of solar radiation on the energy absorbing surface. Higher energy flux on that surface means a smaller surface area for a given total amount of energy and correspondingly reduced thermal losses. Consideration of the energy balances, which are basically similar to those for Flat-plate collectors, shows that operation at higher temperatures is possible. While thermal losses are reduced, two additional kinds of losses become significant: most focusing systems operate only on the beam component of solar radiation, and the diffuse is lost; and additional optical loss terms become significant. A focusing collector can be viewed as a special case of the flat-plate collector, modified by interposition of a radiation concentrator which serves to raise the otherwise low level of radiation on the absorber. Focusing collectors can have radiation intensities at absorbing surfaces increased by a wide range of ratios, from low values of 1.5 to 2, to high values of the order of 10,000. Increasing ratios means increasing temperatures at which energy is delivered

but it also means increasing requirements of precision of optical systems, thus increasing costs.

At the highest range of concentration (and correspondingly highest precision of optics) focusing collectors are termed solar furnaces and are laboratory tools for study of properties of materials at high temperature and similar purposes. Laszlo (1956) and the proceeding of a Solar Furnace Symposium (1957) include extensive discussion of solar furnaces [5], [6].

2. Selective surfaces

An examination of solar collector energy balances shows the desirability of obtaining surfaces with the combination of high absorptance for solar radiation and low emittance for long-wave radiation. This combination of properties is possible to achieve because there is little overlap in wavelength ranges between incoming solar energy (outside the earth's atmosphere 98% is at wavelengths less than 3.00 μm) and emitted long-wavelength radiation (less than 1% is at wavelengths less 3.00 μm for a black surface at 400°k).

The heat balance equation for a surface collecting solar energy can be written as: -

Incident energy = Energy absorbed + Energy Reflected +Energy Transmitted

$$qX = \alpha Xq + (1 - \alpha)Xq, \text{ [7]} \qquad (1)$$

The incident energy represents the solar flux q in watts m^{-2} (which with place and solar time) multiplied by the optical gain X which may be greater or less than unity. The energy absorbed is proportional to the absorptivity α of the surface and this will vary with the spectral distribution of the incident energy but may be defined for a particular wavelength as the function of the total energy absorbed at the wavelength. The remainder of the energy is lost by reflection or by transmission. Most practical solar energy absorbers have a high value of α and negligible transmission, so it is convenient to study more closely the energy absorbed.

Hence our equation may be written: -

$$E_{ex} = E_{ab} - E_{rd} - E_{cv} - E_{cd} \qquad (2)$$

Here E_{ex} is Energy Extracted, E_{ab} is Energy Absorbed, E_{rd} Energy lost by radiation, E_{cv} Energy lost by convection and E_{cd} Energy lost by conduction.

It is obvious from Eq. (2) that a desirable solar energy absorbing surface would maximize α in the solar energy spectrum and minimize ε for the spectral due to the operating temperature of the surface. The concept of a selective surface is shown by consideration of monochromatic reflectance as shown in Figure. 1. This idealized surface is called a Simi grey surface since it can be considered grey in the solar spectrum (i. e., at wavelengths less than about 3.00 μm) and also grey, but with different properties, in the infrared spectrum (i. e. at wavelengths greater than about 3.00 μm) [3].

For this ideal surface, the monochromatic reflectance ρ_λ is very low below a critical or cutoff wavelength λ_c, and very high at wavelengths greater

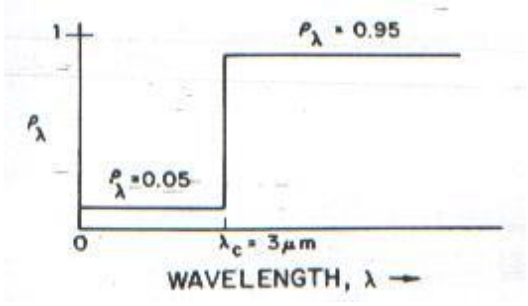

Figure 1. A hypothetical selective surface [3].

than λ_c. Consequently, the absorptivity for solar energy will be very nearly $(1 - \rho_\lambda)$ for $\lambda < 3\ \mu m$. The value of the emissivity will depend on the temperature of the surface, that is, how much of the radiation is emitted at wavelengths greater than λ_c and how much at wavelength less than λ_c.

The values of emittance are usually more sensitive to surface temperature than to wavelength. The wavelength dependence of ρ_λ does not closely approach the ideal curve of Figure.1. Ideal surfaces do not exist. Real selective surfaces do not have a well-defined critical wavelength. Nor do they have uniform properties in the long wave and short wavelengths.

The potential utility of selective surfaces in solar collectors was inferred and further discussed by many researchers [2], [8], [9], [10], [11]. Interest in designing surface with a variety of ρ_λ versus λ characteristics for applications to space vehicles and to solar energy applications resulted in considerable research and compilation of data [12], [13], [14]. Selective surfaces have reviewed and present several recipes for their preparation and performance [11]. Thus, from 1955 on there have been developments which have applicability to solar collectors, and several mechanisms for producing desired combinations of properties have evolved. *Ni* cermet selective absorbers for solar photothermal conversion were introduced and it showed a high efficiency [15]. Choice of selective coating for flat plate collectors was investigated by V. G. Bhide [16]. The performance and stability of some new high-temperature selective absorber systems based on

metal were examined to enhance their performance [17].

Among those of interest in solar energy applications are the following:

1. Coating having high absorptance for solar radiation and high transmittance for long-wave radiation can be applied to substrates with low emittance. Thus, in effect, the coating absorbs solar energy, and the substrate is the (poor) emitter of long-wave radiation. Coating may be homogeneous or have particulate structure; their properties are then either the inherent optical properties of the coating material or of the material properties and the coating structure. Metal oxide coatings on metal substrates which show desirable properties for solar collectors have been developed and used for efficient solar devices [11], [18], [19]. Finely divided lead sulfide coatings were studied by some researchers; the particulate structure of these coatings (as of those of Hottel and Unger) significantly affected the selectivity, and the possibility of a useful selective paint using a vehicle of high transmittance for long-wave radiation was noted [20].

The selective properties of manganese oxide films formed by dipping an Aluminum substrate in an aqueous solution consisting of $KMnO_4$ and HNO_3, have been investigated [21].

2. Interference filters can be applied to low emittance substrates. The filters are formed by depositing alternate layers of metals and dielectrics in quarter wavelength films for the visible and near-infrared. It has been shown that three-layer coatings such as SiO_2-Al-SiO_2 on substrates such as Al should have reflectance less than 0.10 for solar energy and greater than 0.90 for long-wave radiation [12].

The absorptance of AlN-Al (absorbing coating)/Al selective absorbing surfaces, can lining 8-layer AlN-Al composite materials and with distinctive or non-boundaries between the layers, deposited by sputtering technology and heat treated at 400 °C (60 min) is about 0.95 and it's the emittance is close to 0.07 to 0.08 (80 °C) [22].

All-glass evacuated collectors' tube has the configuration of two concentric Borosilicate glass tubes with sputtered Al-N/Al selective surfaces was developed [23].

3. It has been suggested that the surface structure of a metal normally of high reflectance can be designed to make the surface a good absorber of short-wave radiation; this is done by grooving or pitting the surface to create cavities of dimensions near the cutoff wavelength. The surface acts as an assembly of cavity absorbers for short-wavelengths, but for long-wave radiation radiates as a flat surface. The degree of selectivity obtainable by this technique has been limited.

4. "directional selectivity" can be obtained by proper arrangement of the surface on a large scale. Surfaces of deep V-grooves, large relative to all wavelengths of radiation concerned, can be arranged so that radiation from near normal directions to the overall surface will be reflected several times in the grooves, each time absorbing a fraction of the beam. This multiple absorption gives an increase in solar absorptance but at the same time increases the long-wavelength emittance. However, a partially selective surface can have its effective properties substantially improved by proper configuration [24].

The utility of selective surfaces in solar collectors is a function of two major factors.

First, low long-wave emittance is usually obtained at some sacrifice of high solar absorptance, and the net effect of selectivity on performance of a collector (and ultimately on the cost of delivered energy from the collector) must be evaluated for the collector and process in question.

Second, in practice, solar collectors must be designed to operate for many years. The surfaces are usually exposed to oxidizing and corrosive atmospheres and operate more or less elevated temperatures. The data available for α and ε of surfaces are most often available for freshly prepared surfaces.

3. Standard Measuring Procedures

Absorptivity and emissivity are usually calculated from reflectance measurements made with spectrophotometers. A beam of monochromatic radiation is allowed to fall on a sample and the amount reflected is compared with that reflected from a standard surface, since $\alpha_\lambda = 1 - \rho_\lambda$. If directional transmittance equals zero, and K. L. implies that $\varepsilon_\lambda = \alpha_\lambda$, both α_λ and ε_λ can be found for a particular wavelength and directional angle. To obtain total hemispherical reflectance for a particular wavelength and angle of incidence, usually near normal an integrating sphere may be fitted [25]. If an integrating sphere is not used errors can easily occur when calculating hemispherical reflectance from normal reflectance since the angular reflectance distribution of the surface being measured will not be known. Most material, and selective surfaces in particular, are anisotropic with respect to angular reflectance distribution [26].

Two separate spectrophotometers must be used to cover both the solar absorptance and IR emittance

wavelengths. Each set of measurements must be extrapolated somewhat outside of the range of the instrument used since no single detector has a linear response over the entire range of the solar or of the IR emission spectrum.

The reflectance values obtained in this way are integrated over a theoretical solar distribution for a given air mass to calculate solar absorptivity, α. Emittance values are obtained by irradiating the sample with radiation from a heated blackbody and measuring the reflectance with a thermopile detector [27]. However, since there is an intrinsic lowering of reflectance for most surfaces with increasing temperature, it is necessary to provide a means of heating the sample.

Even if all the above equipment were available, the errors involved in using such indirect methods to measure these important parameters make it necessary to look for a simpler approach. Calorimeters are widely used to measure integrated hemispherical emissivity ε, at elevated temperatures. However, the single surface coated flat samples commonly associated with selective surface work are unsuitable for use in these instruments [28].

The above consideration led to the design and production of an instrument which can measure both the absorptivity and emissivity of a selective surface, simply, and under operating conditions directly relevant to those found in an actual solar collector.

4. Principles Of a Solar Calorimeter

The instrument allows the sun's radiation to heat a thermally isolated sample in a vacuum. When the sample reaches stagnated temperature, i.e., when the rate of energy absorbed is equal to the rate of IR emission, the instrument is shaded, and the sample is allowed to cool down. The net rate of heat gain or loss by, or from, the sample is given by

$$\dot{Q} = mC_p\dot{T} \qquad (3)$$

where m is the mass, and C_T is the specific heat at constant volume at temperature T °C.

During heating the rate of temperature rise is a function of emissivity and absorptivity.

The rate of temperature drops while cooling is a function of ε only, so both α and ε can be calculated for the sample surface over a range of temperatures by measuring the thermal changes.

5. Description of The Instrument

A sample is supported on a base made from very high insulation material of thermal wool, of known emissivity 0.87 as shown in Figure. 2. The insulation base was supported on another Aluminum base with thickness about 30 mm, the Aluminum base is pierced from two sides, one of these pierces is for evacuation, and the other is the entrance of the thermocouples. A ring is engraved on the bottom of the Aluminum base and filled with an isolation rubber. A hemi- spherical glass dome of 2mm uniform thickness, has a diameter equals the diameter of the engraved ring, is put on the Aluminum base to cover the sample. The glass dome was obtained by cutting the holder half of a spherical flask. The temperature of the sample, glass dome, and the insulation base are monitored by thermocouples. The thermocouples were connected by the sample, the insulation base and the glass dome. After the connection, the instrument was evacuated by a vacuum pump, then exposed to the sun's radiation to heat up thermally isolated samples in a vacuum. When the sample reached stagnation temperature, the instrument was shaded, and the sample was allowed to cool down. The rate of temperature drops while cooling is a function of emissivity only, then the emissivity can be calculated. When the sample reached the room temperature, the instrument was exposed again to the sun's radiation and the sample heated up again. During heating the rate of temperature rise is a function of emissivity and absorptivity. Absorptivity can be calculated by using the obtained emissivity.

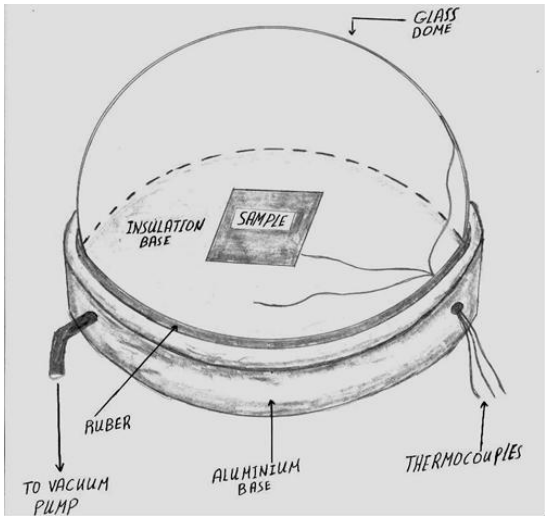

Figure 2. Description of the solar calorimeter.

6. Calculation of Absorptivity and Emissivity:

Electric analogues can be devised to simplify the analysis of radiating exchange processes [29, 30].

We can find formulas for calculating both absorptivity and emissivity by assuming that the thermal exchange in the instrument is between the sample and the hemispherical glass dome, and between the insulation base and the hemispherical

glass dome as shown in Figure 3(i). No thermal radiation exchange between the sample and the insulation base because they are at the same plane. Figure 3(ii). shows the thermal radiation exchange between the hemi-spherical glass dome (g), the sample (s), and the insulation base (b). Each radiating surface has associated with it as a "surface resistance"$(1-\varepsilon)/A\varepsilon$ (A is area) and each pair of surfaces, which each have "space resistance" between them $A_1^{-1}F_{12}^{-1}$ or $A_2^{-1}F_{21}^{-1}$ (F is the shape factor) [29], [31], [32].

The exchange areas A_1F_{12} and A_2F_{21} are equivalent. The electric potential at any knot corresponds to the emissive power per unit area of the respective surface, and currents from the outside connections to the knots represent the rate of heat exchange between the surfaces. So, from Figure 3(ii). we have three surfaces, the insulation base and the sample which are in the same plane and no thermal exchange between them, and the hemispherical glass dome which has thermal exchange between both the sample and the insulation base. Then, the view factors (shape factors) is

$$Fsg = Fb,g = 1 \qquad (4)$$

Network of Figure. (3-3*ii*) will condense to network of Figure 3(iii). by letting

$$r_g = \frac{1-\varepsilon_g}{A_g\varepsilon_g} \qquad (5)$$

$$r_b = \frac{1}{A_bF_{b,g}} + \frac{1+\varepsilon_b}{A_b\varepsilon_b} = \frac{1}{A_b\varepsilon_b} \qquad (6)$$

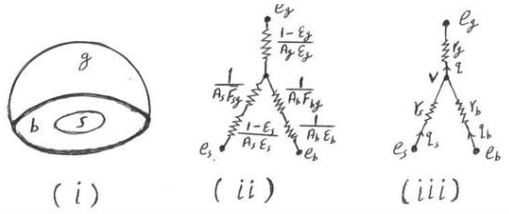

Figure 3. Network analogue for radiation exchange between the sample top and its surroundings.

$$r_s = \frac{1}{A_sF_{s,g}} + \frac{1-\varepsilon_s}{A_s\varepsilon_s} = \frac{1}{A_s\varepsilon_s} \qquad (7)$$

The total rate of heat gain by the glass dome is,

$$\dot{q} = \dot{q}_{s,g} + \dot{q}_{b,g} = \frac{e_s - V}{r_s} + \frac{e_b - V}{e_b} \qquad (8)$$

where, $V = \dot{q}r_g + e_g$

Then, $\dot{q} = \frac{e_s - \dot{q}r_g - e_g}{r_s} + \frac{e_b - \dot{q}r_g - e_g}{r_b} = \frac{e_s}{r_s} - \frac{\dot{q}r_g}{r_s} - \frac{r_g}{r_s} + \frac{e_b}{r_b} - \frac{\dot{q}r_g}{r_b} - \frac{e_g}{r_b}$

Then, $\dot{q}\left(1 + \frac{r_g}{r_s} + \frac{r_g}{r_b}\right) = \frac{1}{r_s}(e_s - e_g) + \frac{1}{r_b}(e_b - e_g)$

$\dot{q}\left(\frac{r_sr_b + r_sr_g + r_br_g}{r_sr_b}\right) = \frac{r_b(e_s-e_g) + r_s(e_b-e_g)}{r_sr_b + r_sr_g + r_br_g}$

Then,

$$\dot{q} = \frac{r_b(e_s - e_g) + r_s(e_b - e_g)}{r_sr_b + r_sr_g + r_br_g} \qquad (9)$$

Using Stefan-Boltzman law of radiation, $e = \sigma T^4$

$e_s - e_g = \sigma(T_s^4 - T_g^4)$ and $e_b - e_g = \sigma(T_b^4 - T_g^4)$

Then Eq. (9) becomes

$$\dot{q} = \frac{\sigma r_b(T_s^4 - T_g^4) + \sigma r_s(T_b^4 - T_g^4)}{r_sr_b + r_sr_g + r_br_g} \qquad (10)$$

Using the value of r_s , r_b and r_g in Eq. (10) we get

$$\dot{q} = \frac{\sigma[A_b^{-1}\varepsilon_b^{-1}(T_s^4 - T_g^{-1}) + A_s^{-1}\varepsilon_s^{-1}(T_b^4 - T_g^4)]}{A_s^{-1}\varepsilon_s^{-1}A_b^{-1}\varepsilon_b^{-1} + A_b^{-1}\varepsilon_b^{-1}(1-\varepsilon_g)A_g^{-1}\varepsilon_g^{-1} + A_s^{-1}\varepsilon_s^{-1}(1-\varepsilon_g)A_g^{-1}\varepsilon_g^{-1}} \qquad (11)$$

The rate of heat loss from the sample to the glass dome is

$$\dot{q}_{s-g} = \frac{e_s - e_g - \dot{q}r_g}{r_s} \qquad (12)$$

Substituting Eq. (10) in Eq. (12) gives

$$\dot{q}_{s-g} = \frac{e_s}{r_s} - \frac{e_g}{r_s} - \frac{r_g}{r_s}\left[\frac{r_b(e_s - e_g) + r_s(e_b - e_g)}{r_sr_b + r_sr_g + r_br_g}\right]$$

$$\dot{q}_{s-g} = \dot{q}_{s-g} = \frac{r_b(e_s - e_g) + r_g(e_s - e_b)}{r_sr_b + r_br_g + r_sr_g} \qquad (13)$$

Since there is no thermal radiation exchange between the sample and the insulation base, then (e_s-e_b=*0*) and Eq. (13) becomes

$$\dot{q}_{s-g} = \frac{r_b(e_s - e_g)}{r_sr_b + r_br_g + r_sr_g} = \frac{r_b\sigma(T_s^4 - T_g^4)}{r_sr_b + r_br_g + r_sr_g} \qquad (14)$$

By using the values of r_s, r_b and r_g Eq. (14) becomes

$$\dot{q}_{s-g} = \frac{\sigma A_b^{-1}\varepsilon_b^{-1}(T_s^4 - T_g^4)}{A_s^{-1}\varepsilon_s^{-1}A_b^{-1}\varepsilon_b^{-1} + A_b^{-1}\varepsilon_b^{-1}(1-\varepsilon_g)A_g^{-1}\varepsilon_g^{-1} + A_s^{-1}\varepsilon_s^{-1}(1-\varepsilon_g)A_g^{-1}\varepsilon_g^{-1}} \qquad (15)$$

By assuming ε_g equal to 1.0 instead of the actual figure of 0.94 for the Pyrex glass dome, Eq. (15) becomes

$$\dot{q}_{s-g} = \sigma A_s\varepsilon_s(T_s^4 - T_g^4) \qquad (16)$$

and Eq. (11) becomes

$$\dot{q} = \sigma[A_s\varepsilon_s(T_s^4 - T_g^4) + A_b\varepsilon_b(T_b^4 - T_g^4)] \qquad (17)$$

The rate of change in temperature of the sample is determined by the heat capacitance of the sample, the incident solar radiation flux, the radiation from the bottom of the sample and the conduction loss through the thermocouple wires. The conduction loss by the thermocouples is very small, then it can

be ignored.

At steady state, heat absorption equals heat loss by conduction, convection, and radiation

Heat losses = Conduction + Convection + Radiation

At steady state, (Absorption = Losses)

$$\alpha_s I_{sol} A_s = hA_s(T_s - T_\infty) + K_{support} A_{contact} \frac{\Delta T}{\Delta L} + I_{IR}$$

where I_{sol} is solar intensity [31].

In the instrument, we get rid of the losses by convection by evacuated the chamber, and we get rid of the losses by conduction by putting an insulation base under the sample, and putting the rubber ring between the glass dome and the Aluminum base, then the heat losses will be only by the thermal radiation,

$$hA_s(T_s - T_\infty) = K_{support} A_{contact} \frac{\Delta T}{\Delta L} = 0$$

Then, $\alpha_s I_{sol} A_s = \sigma A_s T_s^4 \varepsilon_{IR}$

$$\frac{\alpha_s}{\varepsilon_{IR}} = \frac{\sigma T_s^4}{I_{sol}} \quad (18)$$

When the sample is allowed to cool down, the heat stored must be equal to the heat incident minus the heat losses but the heat incident equal to zero, then

$$-\dot{q}_{s-g} = m_s c_{T_s} \frac{dT_s}{dt} = -\sigma A_s \varepsilon_s (T_s^4 - T_g^4)$$

Then the emissivity can be calculated as:

$$\varepsilon_s(T) = \frac{-m_s c_{T_s}}{\sigma A_s (T_s^4 - T_g^4)} \frac{dT_s}{dt} \quad (19)$$

where m_s is the mass of the sample and C_{Ts} is the heat capacitance

As the sample heated up, the heat gain will be the difference between the heat incident and the heat losses.

$$m_s c_{T_s} \frac{dT_s}{dt} = \alpha_s A_s I_{sol} - \sigma[A_s \varepsilon_s (T_s^4 - T_g^4) + A_b \varepsilon_b (T_b^4 - T_g^4)]$$

Then the absorptivity can be calculated as

$$\alpha_s(T) = \frac{m_s c_{T_s} \frac{dT_s}{dt} + \sigma[A_s \varepsilon_s (T_s^4 - T_g^4) + A_b \varepsilon_b (T_b^4 - \text{-}}{A_s I_{sol}} \quad (20)$$

Here $\frac{dT}{dt}$ is not a deferential equation, it is a temperature interval by time interval.

7. METHOD OF THE MEASUREMENT AND RESULTS:

Three thermocouple wires were inserted through one of the bores of the Aluminum base of the instrument. These wires were connected to each the insulation base, the sample and the glass dome. Then the sample was put on the insulation base and covered by the glass dome. The other sides of the wires were connected to thermocouple read out, for monitoring the temperatures of each the sample, the insulation base and the glass dome. To maintain thermal stability and reduce heat transfer due to convection, the instrument is enclosed in a large, partially evacuated glass box, thereby limiting environmental interference. The chamber of the instrument was evacuated by a vacuum pump (10^{-3} Torr). After evacuation, the instrument was exposed to the sun's radiation to heat up the thermally isolated sample in a vacuum. When the sample reached the stagnation temperature, (i.e., the rate of energy absorbed is equal to the rate of IR emission), the instrument was shaded, and the sample was allowed to cool down. While cooling, the temperatures of both the glass dome and the sample were registered for each decreased 10 ºc, as well as time of decreased10 ºc as shown in Table (1), (5) and (9).

The following parameters are used to calculate both ε and α from Eq. 19 and Eq. 20 in Table 1, 3

The mass of the sample m_s= 0.021 *kg*.

The specific heat of the copper C_{Ts} = 383 *J/kg* °*c*.

The area of the sample A_s = 0.01 *m*².

The emissivity of the insulation base (*thermal wool*) ε_b = 0.87.

Stefan-Boltzmann constant $\sigma = 5.669 \times 10^{-8}\, W/m^2K^4$.

The area of the insulation base A_b = 0.021 *m*².

Table 1 The change in temperature of both the sample and the glass dome with respect to time, while cooling, and the results of the emissivity, for the copper selective surface.

T_g ºC	T_s ºC	*Time sec.*	$\varepsilon(T)$ Eq. 19
42	135	-	-
37	130	26	0.296
35	120	62	0.265
33	110	103	0.237
32	100	153	0.221
31	90	215	0.223
29	80	292	0.234
28	70	390	0.225
26	60	516	0.240
25	50	698	0.215
23	40	980	0.205
22	30	1740	0.217

The change in temperature while cooling is plotted in Figure 4., 6. and 8. Eq. (19) then applied for calculating the emissivity of the samples, and the rate of change of temperature (dT/dt) was taken from Figure 4., 6. and 8. as shown in Tables 2., 6., 10.

Table 2 The rate of change in temperature, while cooling, for the copper surface.

T_s °C	dT/dt
130	0.38
120	0.28
110	0.22
100	0.17
90	0.14
80	0.12
70	0.09
60	0.07
50	0.05
40	0.03
30	0.01

When the sample reached the stagnant temperature at cooling (i.e. the sample reached the room temperature), the instrument was exposed again to the sun's radiation and the sample heated up again. While heating, the temperature of the sample, the glass dome and the insulation base is registered for each increased 10 °c, as well as the time of increasing in temperature as shown in Table 3., 7. and 11.

The change in temperature with respect to time, at heating, is plotted as shown in Figure. 5., 7. and 9., and from these figures the rate of change of

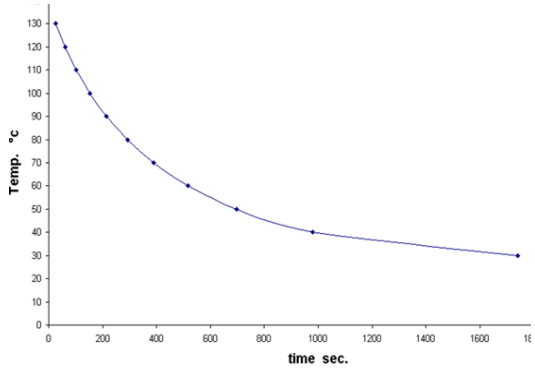

Figure 4 Shows the changing of temperature, while cooling down, with respect to time for the

temperature (dT/dt) was taken when Eq. (20) was applied for calculating the absorptivity of the samples as shown in Tables (4), (8) and (12). The results of both the emissivity and absorptivity as a function of temperature were plotted as shown in Figure. 10., 11. and 12.

The absorptivity and emissivity of three available surfaces had been measured with the instrument. The instrument exposed to the sun radiation at midday (12:30 PM to 3:30 PM). The results, given in Figure 10., 11. and 12., were represented to illustrate the use of the instrument on a flat copper surface coated with aluminum and painted in black (10×10×0.1 cm^3), an Aluminum surface as v-grooving and painted in non-specular black paint (14.5×14.5×0.3 cm^3), and a Graphite sheet which considered as a black surface and as a comparator. Emissivity measurements are independent of the spectral distribution of the incident radiation.

Table 3 The changing in temperature with respect to time, at heating, for the sample, the insulation base and the glass dome, also the results of α and the intensity of the sun's radiation, for the copper selective surface.

T_g °c	T_b °c	T_s °c	*time* sec.	I_{sol} w/m²sec	$\alpha(T)$ Eq.(20)
23	29	30	-	824	0.500
30	51	40	47	824	0.660
32	59	50	78	825	0.790
33	64	60	109	826	0.838
35	68	70	150	830	0.866
36	71	80	195	845	0.898
37	73	90	240	839.8	0.872
38	74	100	330	823	0.880
39	75	110	457	825	0.888
40	77	120	636	840	0.930
41	81	130	885	910	0.973
42	83	135	1200	-	-

The calculation of ε, when extrapolated to room temperature can be seen to lie within the commonly accepted values. The intensities of the solar radiation which applied in Eq. (20), for calculating absorptivity, were measured by (Pyranometer) at the same time of measuring the changing in temperature of the sample at heating.

Table 4 The rate of change of temperature, at heating up, for copper surface

T_s °C	dT/dt
30	0.42
40	0.32
50	0.29
60	0.26
70	0.24
80	0.23
90	0.17
100	0.09
110	0.06
120	0.05
130	0.02

The following parameters are used to calculate both ε and α from Eq. 19 and Eq. 20 in Table 5, 7.

The mass of the sample m_s = 0.03 *kg*. The area of the sample A_s = 0.021 m^2. The specific heat of the Aluminum C_{Ts} = 896 *J/kg °c*.

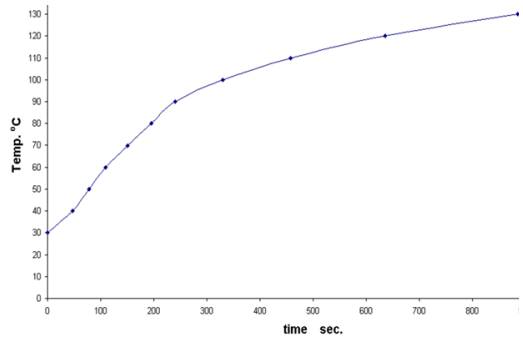

Figure 5 Shows the of temperature, while heating up, with respect to time for the Copper selective sample.

Table 5 The changing in temperature with respect to time, at cooling, for both the sample and the glass, and the results of ε, for the Aluminum selective surface.

T_g °c	T_s °c	time sec.	$\varepsilon(T)$ Eq. (19)
43	90	-	-
35	80	90	0.488
32	70	200	0.423
30	60	355	0.456
28	50	550	0.445
26	40	875	0.440
24	30	1320	0.346

Table 6 The rate of change of temperature, at cooling, for Aluminum surface.

T_s °c	dT/dt
90	0.19
80	0.12
70	0.07
60	0.06
50	0.03
40	0.02
30	0.01

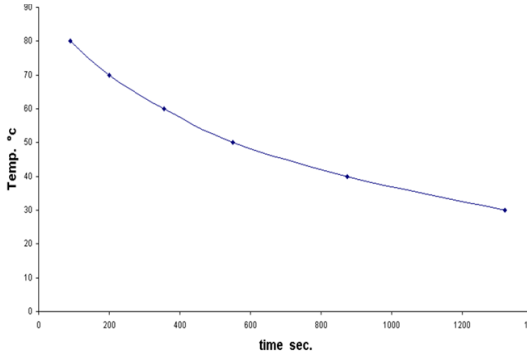

Figure 6 Shows the changing of temperature, while cooling down, with respect to time for the Aluminum sample

Table 7 The changing in temperature with respect to time, at heating, for the sample, the glass and insulation base, and the results of α, and the intensity of sun's radiation, for Aluminum selective surface.

T_g °c	T_b °c	T_s °c	Time sec.	I_{sol} W/m²sec	$\alpha(T)$ Eq. (20)
24	29	30	-	842	0.887
30	50	40	50	835	0.688
32	54	50	105	823	0.600
37	65	60	175	830	0.648
40	68	70	255	825	0.632
41	73	80	380	825	0.633
43	74	90	1140	820	0.612

Table 8 The rate of change of temperature, at heating, for Aluminum surface.

T_s °c	dT/dt
30	0.4
40	0.15
50	0.13
60	0.13
70	0.11
80	0.04
90	0.01

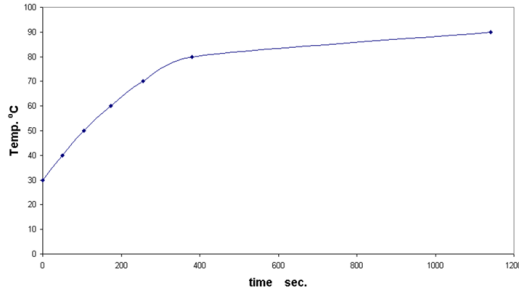

Figure 7 Shows the changing of temperature, while heating up, with respect to time for the Aluminum sample.

The following parameters are used to calculate both ε and α from Eq. 19 and Eq. 20 in Table 9, 11.
The mass of the sample m_s = 0.011 *kg*.
The specific heat of the Graphite C_{Ts} = 710 *J / kg°C*.
The area of the sample A_s = 0.005 m^2.
The area of the insulation base A_b = 0.027 m^2.

Table 9 The changing in temperature with respect to time, at cooling, for both the sample and the glass, for the black surface, and the results of ε.

T_g °C	T_s °C	*time sec.*	$\varepsilon(T)$ Eq. (19)
44	90	-	1.018
36	80	64	0.904
33	70	135	0.879
30	60	210	0.899
29	50	330	0.886
27	40	540	0.774
24	30	1020	0.925

Table 10 The rate of change of temperature, at cooling, for the black surface.

T_s °C	dT/dt
90	0.24
80	0.17
70	0.14
60	0.09
50	0.05
40	0.03
30	0.02

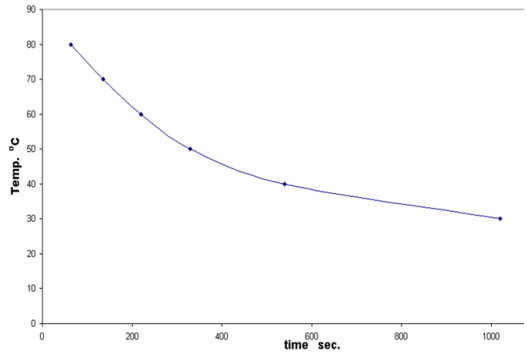

Figure 8 Shows the changing of temperature, while cooling down, with respect to time for the Black body sample.

Table 11 The changing in temperature with respect to time, at heating, for the sample, the glass dome and the insulation base, for the black surface, and also the intensity of the sun's radiation and the results of α.

T_g °C	T_b °C	T_s °C	*time sec.*	I_{sol} *w/m²sec*	$\alpha(T)$ Eq. (20)
24	29	30	-	930	1.076
30	41	40	58	905	0.872
36	50	50	125	935	0.934
42	56	60	202	940	0.954
43	59	70	292	957	0.972
46	63	80	450	953	1.060
47	70	90	1186	958	1.400

Table 12 The rate of change of temperature, at heating, for the black surface.

T_s °C	dT/dt
30	0.33
40	0.2
50	0.15
60	0.11
70	0.08
80	0.03
90	0.02

The absorptivity and emissivity of three surfaces had been measured with the instrument. The results, given in Figures 10., 11. and 12., were represented to illustrate the use of the instrument on a copper coating surface, an Aluminum surface as v-grooving and painted in non-specular black paint, and a Graphite sheet which considered as a black surface and as a comparator. Emissivity measurements are independent of the spectral distribution of the incident radiation.

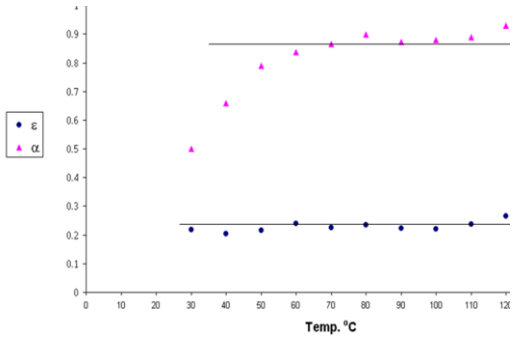

Figure 10 Absorptivity α and emissivity ε for the Copper selective surface**.**

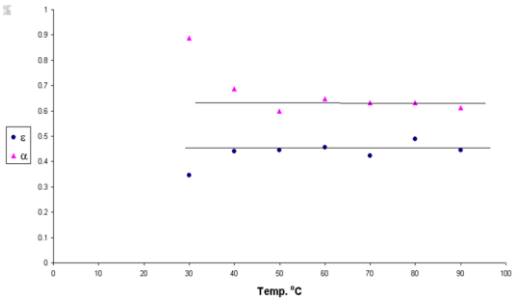

Figure 11 Absorptivity α and emissivity ε for the Aluminum selective surface**.**

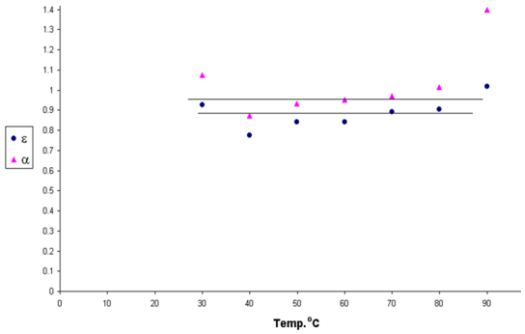

Figure 12 Absorptivity α and emissivity ε for the Black body surface**.**

The calculation of ε, when extrapolated to room temperature can be seen to lie within the commonly accepted values. The intensities of the solar radiation which applied in Eq. (20), for calculating absorptivity, were measured by (Pyranometer at CSES) at the same time of measuring the changing in temperature of the sample at heating.

We note that the first and the last points in

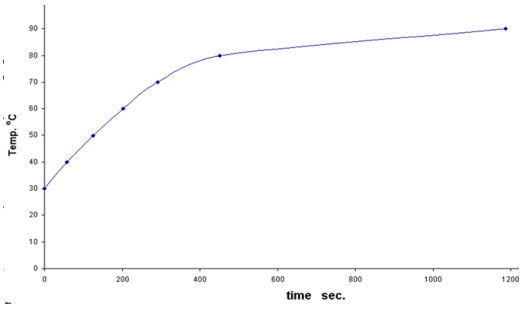

Figure 9 Shows the changing of temperature, while heating up, with respect to time for the Black body sample.

Figures 10., 11. and 12. are not in agreement with the rest of the points, because of dT/dt which applied for calculating both the emissivity and the absorptivity, whereas we take 5 degrees before and after the required point and we cannot do that at the beginning and the end, so these points were omitted from the calculation.

These measurements were done at: CENTER FOR SOLAR ENERGY STUDIES (CSES). Tripoli–Libya.

Conclusion:

Knowledge of the selective radiative properties of the surfaces is essential for the proper design of solar thermal collectors. Although the electromagnetic theory allows the prediction of the radiative properties of pure metals, the calculation becomes very cumbersome for selective surfaces, these being composite material. There are many ways to measure the radiative properties like the spectrophotometers and the calorimeters. The calorimetric methods are widely used to measure the integrated hemispherical emissivities at high temperatures, these ways give essential information for the evaluation of selective surfaces, and the obtained results are directly related to the actual efficiency of performance of a surface under operating conditions.

In this work a calorimeter was designed so that heat transfer by both conduction and convection was nearly suppressed and all heat exchange between the components of the calorimeter occurred essentially by radiation.

In an attempt to calibrate the instrument, a Graphite sheet sample of black surface is used as a black body. Such a sample should have absorptivity and emissivity values very close to 1, the obtained corresponding values are 0.95 and 0.9 respectively. Accordingly, the average absorptivity of the copper selective surface is about 0.9 and we note that it increases by increasing the temperature as shown in Figure 10., but the emissivity is stable at all points, and it is about 0.24. For the Aluminum selective surface, the absorptivity was found to be approximately 0.65 across all measured points, while the emissivity was approximately 0.45.

In contrast, the Copper selective surface exhibits a larger difference between absorptivity and emissivity, which enhances its suitability for solar collector applications. A high absorptivity combined with a low emissivity improves thermal efficiency by maximizing the absorption of incident solar radiation while minimizing radiative heat losses. Consequently, the copper selective surface demonstrates superior performance compared to the Aluminum surface in solar thermal systems.

The calorimeter employed in this study can measure both absorptivity and emissivity of flat samples at elevated temperatures. These measurements can be conducted using either natural solar radiation or a

calibrated solar simulator to ensure controlled and repeatable experimental conditions.

References

[1] F. S. Johnson, "THE SOLAR CONSTANT," *Journal of the Atmospheric Sciences*, vol. 11, no. 6, pp. 431–439, Dec. 1954, doi: https://doi.org/10.1175/1520-0469(1954)011%3C0431:TSC%3E2.0.CO;2.

[2] M. P. Thekaekara and A. J. Drummond, "Standard Values for the Solar Constant and its Spectral Components," *Nature Physical Science*, vol. 229, no. 1, pp. 6–9, Jan. 1971, doi: https://doi.org/10.1038/physci229006a0.

[3] J. A. Duffie, W. A. Beckman, and J. McGowan, "Solar Engineering of Thermal Processes," *American Journal of Physics*, vol. 53, no. 4, pp. 382–382, Apr. 1985, doi: https://doi.org/10.1119/1.14178.

[4] M. J. Kadhim, K. A. Sukkar, and A. S. Abbas, "Electrodepositing of Multi-Layer Ni-Ag Coated by Copper Nanoparticles for Solar Absorber," *Al-Khwarizmi Engineering Journal*, vol. 15, no. 3, pp. 70–83, Sep. 2019, doi: https://doi.org/10.22153/kej.2019.06.009.

[5] T. S. Laszlo, "Solar Furnace in High-Temperature Research," *Science*, vol. 124, no. 3226, pp. 797–800, Oct. 1956, doi: https://doi.org/10.1126/science.124.3226.797.

[6] AbeBooks, "Proceeding of the 1957 Solar Furnace Symposium. The Journal of Solar Energy Science and Energeering. Vol. 1, n. 2-3 by Simon e altri: (1957) | Studio Bibliografico Orfeo (ALAI - ILAB)," *Abebooks.com*, 2026. https://www.abebooks.com/Proceeding-1957-Solar-Furnace-Symposium-Journal/19806574997/bd (accessed Jan. 11, 2026).

[7] H. Messel and S. T. Butler: Solar Energy, *Sydney, Pergamon Press*, 1974.

[8] H. C. Hottel and B. B. Woertz, "The Performance of Flat-Plate Solar-Heat Collectors," *Journal of Fluids Engineering*, vol. 64, no. 2, pp. 91–103, Feb. 1942, doi: https://doi.org/10.1115/1.4018980.

[9] J. T. Gier, and R. V. Dunkle, Transactions of the Conference on the Use of Solar Energy , 2, Part I, 41, U. of Arizona Press, 1958. "Selective Spectral Characteristics as an Important Factor in the Efficiency of Solar Collectors."

[10] Tabor, H., Bull. Res. Coun. Israel, 5A, No. 2, 119 (January 1956). "Selective Radiation".

[11] H. Tabor, "Solar Collectors, Selective Surfaces, and Heat Engines," *Proceedings of the National Academy of Sciences of the United States of America*, vol. 47, no. 8, pp. 1271–1278, 1961, doi: https://doi.org/10.2307/71020.

[12] Martin, D. C. and Bell, R., Proceedings of the Conference on Coatings for the Aerospace Environment, WADD-TR-60-TB, Wright Air Development Division, Dayton, Ohio (November 1960). "The Use of Optical Interference to Obtain Selective Energy Absorption".

[13] Edwards, D. K., Nelson, K. E., Roddick, R. D., and Gier, J. T., Report No. 60-93, Dept. of Engineering, univ. of California (October 1960). "Basic Studies on the Use and Control of Solar Energy".

[14] Schmidt, R. N., Park, K. C., and Janssen, E., Tech. Doc. Report No. ML-TDR-64-250 from Honeywell Research Center to Air Force Materials Laboratory (September 1964). "High Temperature Solar Absorber Coatings, Part II".

[15] M. Okuyama, K. Furusawa, and Y. Hamakawa, "Ni cermet selective absorbers for solar photothermal conversion," *Solar Energy*, vol. 22, no. 6, pp. 479–482, 1979, doi: https://doi.org/10.1016/0038-092x(79)90019-7.

[16] V. G. Bhide, J.S. Vaishya, V. K. Nagar, and S. K. Sharma, "Choice of selective coating for flat plate collectors," *Solar energy*, vol. 29, no. 6, pp. 463–465, Jan. 1982, doi: https://doi.org/10.1016/0038-092x(82)90054-8.

[17] J. H. Schön, G. Binder, and E. Bucher, "Performance and stability of some new high-temperature selective absorber systems based on metal/dielectric multilayers," *Solar Energy Materials and Solar Cells*, vol. 33, no. 4, pp. 403–416, Aug. 1994, doi: https://doi.org/10.1016/0927-0248(94)90001-9.

[18] H. C. Hottel and T. A. Unger, "2 The properties of a copper oxide aluminum selective black surface absorber of solar energy," *Solar Energy*, vol. 3, no. 3, pp. 10–15, Oct. 1959, doi: https://doi.org/10.1016/0038-092x(59)90134-3.

[19] P. Kokoropoulos, E. Salam, and F. Daniels, "Selective radiation coatings. Preparation and high temperature stability," *Solar Energy*, vol. 3, no. 4, pp. 19–23, Dec. 1959, doi: https://doi.org/10.1016/0038-092x(59)90003-9.

[20] D. A. Williams, T. A. Lappin, and J. A. Duffie, "Selective Radiation Properties of Particulate Coatings," *Journal of Engineering for Power*, vol. 85, no. 3, pp. 213–220, Jul. 1963, doi: https://doi.org/10.1115/1.3675262.

[21] H. S. Al-Jumaili, A. A. J. Al-Douri, and I. N. Al-Naimi, "Optical selectivity of manganese oxide film,"*Renewable Energy*, vol. 1, no. 2, pp. 219–222, Jan. 1991, doi: https://doi.org/10.1016/0960-1481(91)90078-

4.
[22] Y. Shi and X. Yang, "Selective absorbing surface for evacuated solar collector tubes," *Renewable Energy*, vol. 16, no. 1–4, pp. 632–634, Jan. 1999, doi: https://doi.org/10.1016/s0960-1481(98)00240-7.
[23] Z. Yin, Z. Xue, J. Zhang, and C. Shen, "Graded Al-N/Al absorbing surfaces for all-glass evacuated tubular collectors — R, D and production: Bridging the gap," *Renewable Energy*, vol. 16, no. 1–4, pp. 624–627, Jan. 1999, doi: https://doi.org/10.1016/s0960-1481(98)00238-9.
[24] K. G. T. Hollands, "Directional selectivity, emittance, and absorptance properties of vee corrugated specular surfaces," *Solar Energy*, vol. 7, no. 3, pp. 108–116, Jul. 1963, doi: https://doi.org/10.1016/0038-092x(63)90036-7.
[25] R. V. Dunkle, D. K. Edwards, J. T. Gier, and J. T. Bevans, "Solar reflectance integrating sphere," *Solar Energy*, vol. 4, no. 2, pp. 27–39, Apr. 1960, doi: https://doi.org/10.1016/0038-092x(60)90112-2.
[26] E. Schmidt and E. Eckert, "Über die Richtungsverteilung der Wärmestrahlung von Oberflächen," *Forschung auf dem Gebiete des Ingenieurwesens*, vol. 6, no. 4, pp. 175–183, Jul. 1935, doi: https://doi.org/10.1007/bf02578830.
[27] J. T. Gier, R. V. Dunkle, and J. T. Bevans, "Measurement of Absolute Spectral Reflectivity from 10 to 15 Microns," *Journal of the Optical Society of America*, vol. 44, no. 7, pp. 558–558, Jul. 1954, doi: https://doi.org/10.1364/josa.44.000558.
[28] H. Willrath and R. B. Gammon, "The measurement of optical properties of selective surfaces using a solar calorimeter," *Solar Energy*, vol. 21, no. 3, pp. 193–199, 1978, doi: https://doi.org/10.1016/0038-092x(78)90021-x.
[29] V. T. Sinha, "Heat transfer, J. P. Holman, McGraw-Hill, New York(1972). 462 pages." *AIChE Journal*, vol. 18, no. 6, pp. 1280–1280, Nov. 1972, doi: https://doi.org/10.1002/aic.690180643.
[30] https://gyansanchay.csjmu.ac.in/wp-content/uploads/2022/01/CHE-S204-Chapter-8-Radiation_G5.pdf.A. K. Oppenheim, "Radiation Analysis by the Network Method," *Transactions of the American Society of Mechanical Engineers*, vol. 78, no. 4, pp. 725–735, May 1956, doi: https://doi.org/10.1115/1.4013795.
[31] E. M. Sparrow, R. D. Cess, and E. Schmidt, "Radiation Heat Transfer," *Journal of Applied Mechanics*, vol. 34, no. 4, pp. 1055–1055, Dec. 1967, doi: https://doi.org/10.1115/1.3607834